

Acetylcholinesterase-transgenic mice display embryonic modulations in spinal cord choline acetyltransferase and neurexin I β gene expression followed by late-onset neuromotor deterioration

(neuromuscular junction/motoneurons)

CHRISTIAN ANDRES*^{†‡}, RACHEL BEERI*[‡], ALON FRIEDMAN*, EFRAT LEV-LEHMAN*, SIVAN HENIS*, RINA TIMBERG*, MOSHE SHANI[§], AND HERMONA SOREQ*[¶]

*Department of Biological Chemistry, The Hebrew University of Jerusalem, 91904 Israel; and [§]Department of Molecular Genetics, Agricultural Research Organization, The Volcani Center, Bet Dagan, 50250 Israel

Communicated by Roger D. Kornberg, Stanford University School of Medicine, Stanford, CA, May 9, 1997 (received for review March 12, 1997)

ABSTRACT To explore the possibility that overproduction of neuronal acetylcholinesterase (AChE) confers changes in both cholinergic and morphogenic intercellular interactions, we studied developmental responses to neuronal AChE overexpression in motoneurons and neuromuscular junctions of AChE-transgenic mice. Perikarya of spinal cord motoneurons were consistently enlarged from embryonic through adult stages in AChE-transgenic mice. Atypical motoneuron development was accompanied by premature enhancement in the embryonic spinal cord expression of choline acetyltransferase mRNA, encoding the acetylcholine-synthesizing enzyme choline acetyltransferase. In contrast, the mRNA encoding for neurexin-I β , the heterophilic ligand of the AChE-homologous neuronal cell surface protein neuroligin, was drastically lower in embryonic transgenic spinal cord than in controls. Postnatal cessation of these dual transcriptional responses was followed by late-onset deterioration in neuromotor performance that was associated with gross aberrations in neuromuscular ultrastructure and with pronounced amyotrophy. These findings demonstrate embryonic feedback mechanisms to neuronal AChE overexpression that are attributable to both cholinergic and cell–cell interaction pathways, suggesting that embryonic neurexin I β expression is concerted *in vivo* with AChE levels and indicating that postnatal changes in neuronal AChE-associated proteins may be involved in late-onset neuromotor pathologies.

Accumulated and compelling cell culture evidence increasingly points to noncatalytic morphogenic roles for acetylcholinesterase (AChE), the enzyme known for its function in terminating neurotransmission at cholinergic synapses by hydrolysis of acetylcholine (ACh) (1–3). At the *in vivo* milieu, we reported a morphogenic activity for overexpressed human AChE in developing amphibian neuromuscular junctions (NMJs) (4, 5). This activity was attributed primarily to modulations in synaptic acetylcholine levels and consequent changes in cholinergic neurotransmission. However, the high degree of sequence homology between AChE and a family of nervous system cell surface proteins suggests that AChE also might be involved in cell adhesion processes recruited during synaptogenesis and long-term synapse maintenance. Proteins participating in these processes include mammalian neuroligins (6, 7), *Drosophila* neurotactin (8), and gliotactin (9). Recently, a chimera in which the extracellular cholinesterase-

like domain of neurotactin was replaced with the homologous domain from *Torpedo* AChE was reported to retain ligand-dependent cell-adhesive properties similar to the native molecule (10). This reinforced the notion that AChE may play a role in neuronal cell adhesion.

In mammals, the AChE-homologous neuroligins were identified as heterophilic ligands for a splice-site specific form of the synapse-enriched neuronal cell surface protein neurexin I β (11). Neurexins represent a family of three homologous genes (I, II, and III), giving rise to α and β forms that can undergo further alternative splicing to generate over 1,000 isoforms (12). Neurexins, as AChE, are expressed in postmitotic neurons of the embryonic nervous system, including spinal cord, before synaptogenesis (13). The wealth of alternative splicing patterns predicted for both the neurexins and the neuroligins, together with their spatio-temporally restricted expression patterns, have led to the suggestion that they could mediate an almost infinite number of highly specific cell-cell interactions in the nervous system (12, 13). This raises the possibility that AChE, by virtue of its homology to neuroligin, could play a role in neurexin-mediated cell-adhesion interactions. To explore this issue, we asked whether overexpression of AChE might feed back upon expression of neurexins *in vivo* and searched for potential correlations between AChE overexpression and changes in synapse development and maintenance. For this purpose, we chose to study the NMJ and its innervating motoneurons in transgenic mice expressing human AChE in brain and spinal cord (14). Our observations correlate neuronal overexpression of AChE with embryonic feedback mechanisms attributable to both cholinergic and noncholinergic pathways. They also suggest that postnatal changes in neuronal AChE and/or its associated proteins may play a role in late-onset neuromotor pathologies.

EXPERIMENTAL PROCEDURES

PCR Analyses. PCR was performed essentially as described previously (14) using species-specific primers assigned to nucleotides 1,522 (+) and 1,797 (–) in exons 3 and 4 of the human AChE cDNA, nucleotides 375 (+), 1,160 (–) in exons 2 and 3 of the mouse AChE gene (15), nucleotides 83 (+), 646 (–) of the mouse choline acetyltransferase (CHAT) gene (16),

Abbreviations: ACh, acetylcholine; AChE, acetylcholinesterase; ChAT, choline acetyltransferase; NMJ, neuromuscular junction; RT-PCR, reverse transcription-PCR.

[†]Present address: Laboratoire de Biochimie et de Biologie Moléculaire, Centre Hospitalier Régional Universitaire, INSERM U 316, 37044 Tours Cedex, France.

[‡]C.A. and R.B. contributed equally to this study.

[¶]To whom reprint requests should be addressed. e-mail: Soreq@shum.huji.ac.il.

The publication costs of this article were defrayed in part by page charge payment. This article must therefore be hereby marked “advertisement” in accordance with 18 U.S.C. §1734 solely to indicate this fact.

© 1997 by The National Academy of Sciences 0027-8424/97/948173-6\$2.00/0 PNAS is available online at <http://www.pnas.org>.

nucleotides 822 (+), 996 (-) of the mouse β -actin gene (17), nucleotides 978 (+) and 1,113 (-) of the neurexin I β gene (12), and nucleotides 1,179 (+) and 1,450 (-) of the neurexin III β gene (12). Resultant PCR products (276, 786, 564, 174, 136, and 272 bp, respectively) obtained from similar amounts of RNA were removed and analyzed on ethidium bromide-stained agarose gels.

High-Resolution *In Situ* Hybridization. Hybridization was done essentially as described (17) with the following modifications: Tissues were fixed in 4% paraformaldehyde/0.1% glutaraldehyde (2 hr) and washed at 4°C. Clearing in 6% H₂O₂ (1 hr) was followed by proteinase K (10 μ g/ml, 15 min), glycine (2 mg/ml, 20 min), and refixation (4% paraformaldehyde/0.2% glutaraldehyde, 20 min), all in PBS/0.1% Tween-20. Hybridization buffer and washing solutions included 1% SDS. Hybridization was 16 hr at 52°C with 50-mer, 5'-biotinylated, 2-O-methyl cRNA probes (10 μ g/ml) (Microsynth, Switzerland) directed to the following sequences: AChE mRNA: mouse exon 6, positions 1,932–1,981 (15); mouse exon 5, positions 249–199 (18); and mouse ChAT cRNA, positions 553–602 (16). Posthybridization washes were at 56°C.

Staining Procedures and Microscopy. Diaphragm muscles were fixed *in situ* with 4% paraformaldehyde/0.1% glutaraldehyde solution in PBS for 5 min at room temperature, dissected, refixed for 2 hr, and kept at 4°C in PBS until used. AChE activity staining was for 5 min at room temperature as previously described (14). Fifty-micrometer-thick, paraformaldehyde/glutaraldehyde-fixed spinal cord sections were stained for 30 min. Electron microscopy on 80-nm-thick sections and morphometric analyses were essentially as described (5). Student's *t* test was used to evaluate morphometric data.

AChE Activity Measurements. Acetylthiocholine hydrolysis levels were determined spectrophotometrically in the presence of 10⁻⁵ M of the selective butyrylcholinesterase inhibitor iso-OMPA (tetraisopropylpyrophosphoramidate). Enzyme-antigen immunoassay was as described (5).

Electromyography. After dissection of the hindleg, a tungsten bipolar stimulating electrode was positioned on the trunk of the sciatic nerve and evoked muscle fiber potentials recorded by a microelectrode placed on the gastrocnemius muscle. The nerve was stimulated by brief (0.1 msec) stimuli at increasing intensities (<1 mA). Data were recorded through an AC-DC amplifier (A-M Systems, Everett, WA, model 1800), digitized on line, and analyzed using Pclamp 6.0 (Axon Instruments, Foster City, CA). Muscle temperature, maintained at 32 \pm 1°C by a warming lamp, was continuously monitored. In each animal, about 10 different recordings were taken. Anesthesia was accomplished with intraperitoneal administration of Nembutal (60 mg/kg weight).

Grip Test. Mice were suspended by their forelegs on a 3-mm-thick horizontal rope 1 m above bench level. The time it took them to grip the rope with their hindlegs (escape latency) was measured three times at 1-min intervals for sex-matched mice with similar body weights. Unsuccessful trials and those that ended in animals falling off the rope were recorded as 10 sec.

RESULTS

Human AChE from Spinal Cord Motoneurons Reaches Transgenic Muscle. AChE-transgenic mice carry, and express in their central nervous system (14), the synaptic form (5) of human AChE. Reverse transcription-PCR (RT-PCR) demonstrated expression of human AChE mRNA in spinal cord, but not in muscle (Fig. 1A) of AChE-transgenic mice. High-resolution *in situ* hybridization using a biotinylated 2-O-methyl cRNA probe detected both mouse and human AChE mRNA transcripts throughout neuronal perikarya within the anterior horn of the spinal cord in both control and transgenic adult mice (Fig. 1B and C). Large polygonal neurons with the

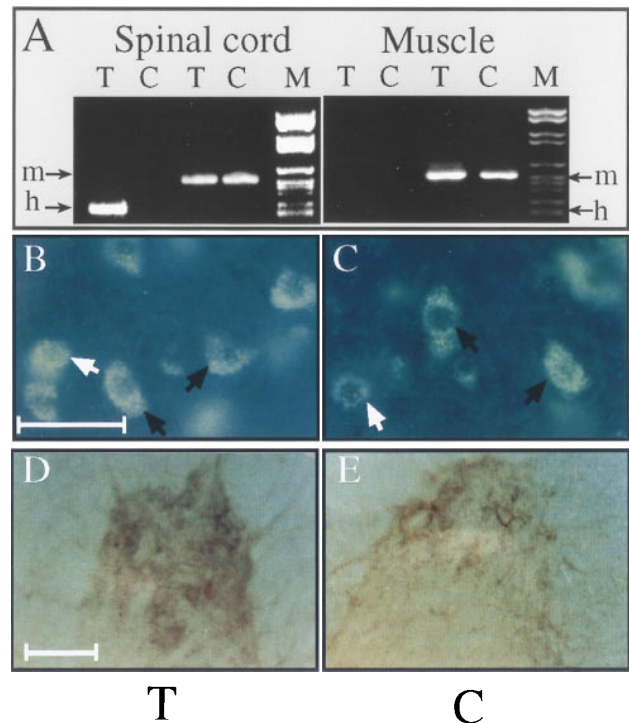


FIG. 1. Human AChE cDNA is expressed in spinal cord neurons but not muscle. (A) RT-PCR analyses. Primers specific for mouse (m) or human (h) AChE mRNA indicates expression of the transgene in transgenic (T) spinal cord, but not muscle. Control (C) mice express the endogenous mRNA in both tissues. (B and C) *In situ* hybridization. A probe detecting both mouse and human AChE mRNAs labeled neurons in 50- μ m cervical spinal cord sections from both transgenic (B) and control (C) mice. Black arrows indicate large polygonal α motoneurons; white arrows indicate γ motoneurons and/or interneurons. ELF kit 6605 (Molecular Probes) diluted 1:250 was used for detection. (Size bar, 50 μ m.) Note that labeling is restricted to cells with neuronal morphology. (D and E) Enzyme activity. Fixed sections from the anterior horn of lumbar spinal cord of transgenic (D) or control (E) mice were cytochemically stained for catalytically active AChE. Note the enhanced activity in nerve fibers and cell bodies from the transgenic spinal cord. (Size bar, 100 μ m.)

characteristic features of α motoneurons as well as small round cells resembling γ motoneurons or interneurons, but not cells with glial morphology, were labeled (Fig. 1B and C). Similar patterns of AChE mRNA labeling were observed in the cervical, lumbar, and dorsal regions of the spinal cord (data not shown). Cytochemical staining revealed AChE activity in neuronal processes within adult transgenic spinal cord, high above levels observed in controls (Fig. 1D and E). Overexpression of AChE in spinal cord was confirmed by quantitative assays demonstrating approximately 25% higher activity in spinal cord extracts from transgenic animals. Using a human AChE-specific mAb (mAb 101-1) in an enzyme-antigen immunoassay, this difference was attributed to AChE of human origin evenly distributed between the salt and detergent-soluble fractions. In light of reports that motoneurons contribute to synaptic AChE at the amphibian NMJ (19) we considered the possibility that AChE of human origin might be present at the NMJ despite the apparent transcriptional silence of the human gene in muscle. In detergent muscle extracts, no significant difference in total AChE activity was observed between six control and seven transgenic adult mice (33.4 \pm 6.9 vs. 35.9 \pm 1.3 nmol/min per mg of protein, respectively). However, the binding of up to 6% of the total enzyme to mAb 101 indicated the presence of a minor fraction of human AChE in muscle (data not shown).

Spinal Cord Neurons of Embryonic and Newborn Transgenic Mice Display Drastic Changes in ChAT and β -Neurexin

mRNAs. To search for potential changes in gene expression accompanying overexpression of AChE in spinal cord, we performed semiquantitative, kinetic RT-PCR. PCR signals reflected similar levels of human AChE mRNA in spinal cord of embryonic day 17 (E17), newborn, and 5-week-old mice (Fig. 2A). In contrast, mouse AChE mRNA was hardly detectable in the spinal cord before birth, but increased approximately 8-fold in newborn mice, and continued to increase in young adults, all in both groups (Fig. 2A). As excess AChE is expected to reduce the bioavailability of ACh and suppress cholinergic neurotransmission, we searched for potentially compensatory changes in expression of the ACh-synthesizing enzyme ChAT. RT-PCR demonstrated premature embryonic expression of ChAT mRNA at E17 in transgenic, but not control, spinal cord (Fig. 2A). In newborn mice, a smaller, but still apparent, enhancement in ChAT mRNA levels was observed in transgenic as compared with control mice. However, at 5 weeks transgenic and control mice displayed similar levels of this transcript. Actin mRNA levels, which served as a control for the integrity and amounts of mRNA in these preparations, remained unchanged throughout development (data not shown).

Transgenic, but not control, embryonic spinal cord neurons were intensively labeled in *in situ* hybridization with an AChE cRNA probe recognizing both human and mouse AChE mRNAs (Fig. 2B). In contrast, a probe selective for mouse AChE yielded fainter labeling and no significant difference between transgenic and control motoneurons (Fig. 2B). Significantly, a mouse ChAT cRNA probe prominently labeled motoneuron perikarya in transgenic, but not control, spinal cord (Fig. 2B). Thus, enhanced signals in both RT-PCR and *in situ* hybridization indicated augmented neuronal ChAT

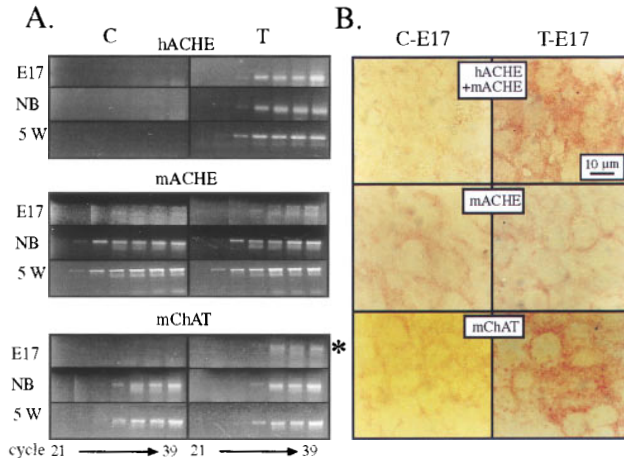


FIG. 2. Transgenic human AChE (hAChE) mRNA expression induces a transient embryonic enhancement in ChAT mRNA levels. (A) RT-PCR analyses. RNA extracted from spinal cord of control (C) and transgenic (T) mice at the noted ages was subjected to kinetic RT-PCR using primers for the noted mRNAs (see *Experimental Procedures*). Aliquots of amplified DNA representing human (h) or mouse (m) AChE or ChAT mRNAs were removed every third cycle from cycle 21, representing differences of *ca.* 8-fold between samples. Products were electrophoresed and stained with ethidium bromide. Note that hAChE mRNA is present only in transgenic mice, that endogenous AChE mRNA levels are similar in control and transgenic animals, and that while mChAT levels are undetectable in control E17 embryos, a prominent signal, marked by an asterisk, is observed in transgenic embryos. In postnatal mice, ChAT mRNA levels in transgenic and control spinal cord are indistinguishable. NB, newborn. (B) *In situ* hybridization. Seven-micrometer sections from the lumbar spinal cord of control (C) and transgenic (T) E17 embryos were subjected to *in situ* hybridization. Fast-red (Boehringer Mannheim) served for detection. Note the intense AChE and ChAT mRNA signals in transgenic cell bodies.

mRNA levels in transgenic mice. At subsequent ages, however, no such differences could be detected, pointing at the transient nature of this embryonic feedback response. In light of the considerable homologies between AChE and the neurexin β ligand neuroligin (7), we further looked for changes in the expression of neurexin β in spinal cord of transgenic mice. Both embryonic and newborn, but not 5-week-old, transgenic mice displayed drastically reduced levels of neurexin $I\beta$ compared with controls (Fig. 3), suggesting that neurexin-neuroligin relationships would be altered in the transgenic spinal cord and indicating that the accessibility of AChE-like domains affects neurexin $I\beta$ production. In contrast, neurexin $III\beta$ levels were barely detectable in either group at these ages and similar to each other at 5 weeks. Actin mRNA levels, as measured by RT-PCR, were identical in both groups at all ages.

Transgenic AChE Expression Induces Persistent Enlargement of Motoneurons. The total number and spatial distribution of motoneurons in transgenic spinal cord was essentially normal, suggesting that human AChE expression did not affect neuronal proliferation or migration and did not cause neuronal death. However, measurements of cell area revealed age-dependent changes in morphology among anterior horn neurons from transgenic as compared with control mice. Neuronal cell bodies in control embryos averaged $44.5 \pm 15.8 \mu\text{m}^2$ in size (mean \pm SD) whereas transgenic neurons displayed areas of $51.5 \pm 13.5 \mu\text{m}^2$ (Fig. 4A) ($P < 0.05$, Student's *t* test). Postnatal maturation of spinal cord neurons was accompanied by dissociation into two distinct populations, one consisting of small neurons ($25\text{--}150 \mu\text{m}^2$) likely to be interneurons and γ motoneurons, and the other of large neurons ($>150 \mu\text{m}^2$) that includes the α motoneurons. There was no difference between postnatal control and transgenic spinal cord in either the number or the perikaryal area of the small neurons. Similarly, the fraction of neurons larger than $150 \mu\text{m}^2$ was similar in transgenic and control mice (data not shown), suggesting normal lineage distribution of spinal cord motoneurons. Nevertheless, transgenic motoneurons were significantly enlarged relative to controls, with perikarya of $220 \mu\text{m}^2$, as compared with $160 \mu\text{m}^2$ ($P < 0.02$, Fig. 4B). The normal size and unmodified staining of nuclei suggested that the enlarged neurons were viable in both embryonic and adult spinal cord

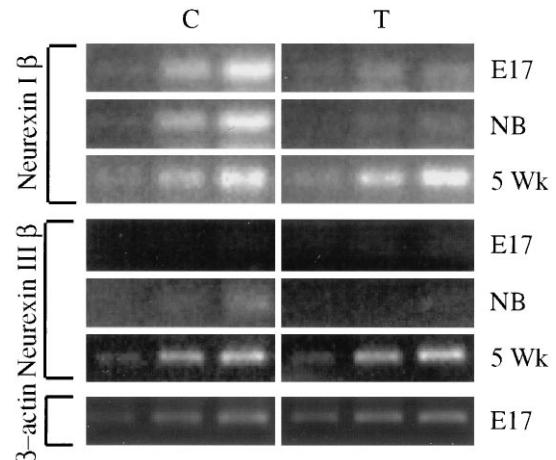


FIG. 3. Neurexin $I\beta$ mRNA is dramatically suppressed in embryonic and newborn transgenic mice. Primers specific for neurexin $I\beta$ and $III\beta$ mRNAs (see *Experimental Procedures*) were used in semiquantitative RT-PCR on spinal cord RNA from control (C) and transgenic (T) mice at the noted ages. Note the dramatic reduction in signal intensities for neurexin $I\beta$ in embryonic (E17) and newborn (NB) transgenic mice compared with controls and to 5-week-old (5 Wk) mice. Primers for β -actin mRNA served to verify quantity and quality of RNA in each sample. Shown are PCR products sampled every third cycle (i.e., reflecting 8-fold differences) from cycle 21 for β -actin and cycle 24 for neurexins.

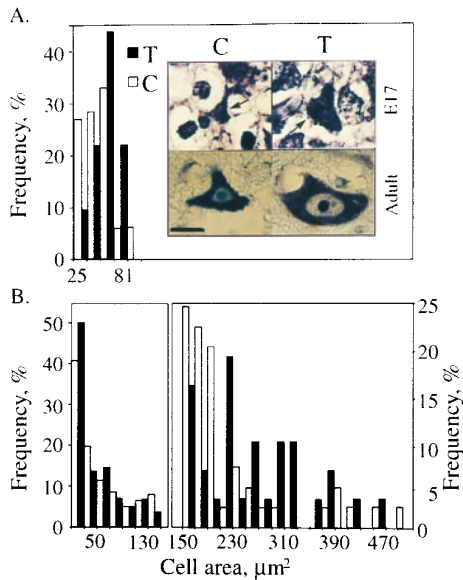


FIG. 4. AChE overexpression is associated with enlarged motoneuron perikarya. (A) Embryonic enlargement. Thoracic spinal cord sections from E17 transgenic (T) and control (C) mice were stained with cresyl violet, and the perikaryal areas in μm^2 of ventral horn cells measured. Presented are percent fractions of the total number of cresyl violet positive cells in each size group (67 control and 32 transgenic cells were measured). This analysis revealed overall enlargement of neurons in transgenic embryonic spinal cord ($P < 0.05$). (Inset) Representative cresyl violet-positive control (C) and transgenic (T) neurons from embryonic (E17) and 3-month-old (adult) mice are presented. Note that the enlarged neurons characteristic of transgenic animals maintain the normal polygonal morphology. (Size bar, $10 \mu\text{m}$.) Arrows indicate motoneurons. (B) Adult enlargement. Separate size distributions for ventral horn neurons up to $150 \mu\text{m}^2$ (Left) and larger than $150 \mu\text{m}^2$ (Right) from adult mice are presented. Smaller cells (202 control and 186 transgenic cells), presumably interneurons and γ -motoneurons, showed similar perikaryal area distributions in transgenic and control animals. In contrast, the larger ventral horn cells, presumably α -motoneurons (44 control and 27 transgenic cells), preserved the embryonic trend of enlarged perikarya observed in transgenic animals ($P < 0.02$).

(Fig. 4A, Inset). We found no examples for such selective neuronal enlargement in neurodegenerative diseases.

AChE-Induced Progressive Impairments in Neuromuscular Function. Transgenic animals developed normally and acquired normal motor functions at the same ages as control mice. Adult transgenic mice walked normally, with track width and pace length similar to those of controls (not shown). Swimming speed of 4-month-old transgenic mice (21.4 ± 4.0 m/min) was only slightly slower than controls (25.0 ± 4.0 m/min) ($n = 10$). However, transgenic animals exhibited severely impaired performance in a rope grip test designed to test coordinated sensorimotor activity of the abdomen, back, and leg muscles (Fig. 5A). When hung on the rope, transgenic mice acquired a loose, weakened posture, and 4-month-old transgenic, but never control, mice fell off the rope altogether in 20% of 30 sessions with 10 animals. Weakness in the grip test was already evident as a >2 -fold difference in escape latency ($P < 0.02$) at the age of 4 weeks, but worsened ($P < 0.01$) by 4 months of age.

Transgenic AChE Expression Leads to Electromyographic Abnormalities. The intensity of compound action potentials recorded on the surface of the sciatic nerve did not differ between control and transgenic adult mice. Nerve conduction velocity was normal, and no late potentials were detected, suggesting normal myelination and number of axons (data not shown). In addition, direct recording from the gastrocnemius muscle did not reveal spontaneous denervation activity. Nev-

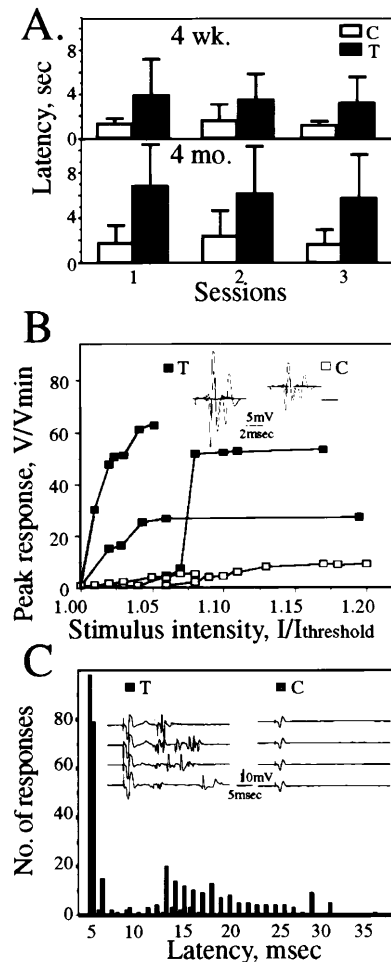


FIG. 5. Postnatal motor function impairments worsen with age. (A) Grip test performance. Groups of 5–10 mice at the ages of 4 weeks and 4 months [transgenic (T) and control (C)] were suspended with their forelegs on a 3-mm diameter rope and the time taken to securely grip the rope with their hindlegs was noted (latency) (see *Experimental Procedures*). Presented are escape latencies in seconds (average \pm SD). Note the slower performance of transgenics as compared with controls at both age groups and the worsening of this phenotype with age. (B) Electromyographic profiles. Evoked muscle fiber potentials (V/Vmin) after sciatic nerve stimulation were recorded by a microelectrode placed on the surface of the gastrocnemius muscle in three transgenic (■) and three control (□) mice. (Inset) Superposition of responses evoked by increasing stimulus intensity up to 1.0 mA at 1 Hz as in the enclosed scale. Saturation of response occurred only at high stimulus intensities and required more stimuli in transgenics than in controls. Note that in the transgenic muscle several negative peaks were observed in response to a single stimulus. (C) Delayed repetitive firing of action potentials. After 100 supramaximal stimulations at 1 Hz, abnormal late potentials (filled bars) appeared in four transgenic animals for up to 40 msec poststimulation as compared with a few signals in four control animals (empty bars). Presented are numbers of response spikes as a function of latency time for 10 different measurements.

ertheless, evoked potentials recorded from the gastrocnemius muscle fibers in response to stimulation of the common trunk of the sciatic nerve disclosed three main abnormalities. In control animals, a small increase in stimulus intensity induced small and gradual increases in the amplitude of the muscle's compound action potential, so that supramaximal response amplitudes were up to 10-fold greater than the threshold response. In transgenic animals, parallel increases in stimulus intensity triggered considerably larger jumps in the amplitude of the action potentials. These observations indicated enlargement of functional motor units and an increased number of

muscle fibers recruited by the stimulated axons (Fig. 5*B*). Moreover, muscle potentials in transgenic mice were of greater amplitude and duration than those in controls, with frequent multipeaked shapes (mainly three subpeaks) rarely seen in controls (Fig. 5*B* and *C*). Finally, repetitive supramaximal stimulations at 1 Hz induced pathological late potentials (latency up to 40 msec), which appeared frequently in transgenic animals but very rarely in controls (Fig. 5*C*). In 2 of 4 cases, 3-Hz stimulations after tetanization by 300 stimulations at 30 Hz resulted in myasthenia-like decreases (>10%) in the intensity of responses in transgenic, but not in control animals (data not shown). These observations suggested disturbed neuromuscular communication in adult AChE-transgenic mice.

NMJs and Muscles of Transgenic Animals Undergo Dramatic Morphological Changes. Adult AChE-transgenic mice developed diaphragm motor endplates that were 60% larger, on average, than controls (Fig. 6*A*). Therefore, over half of the transgenic endplates examined, but only 10% of controls, were larger than 600 μm^2 . In addition, transgenic endplates failed to display the complex boundaries found in control endplates, but acquired a simple ellipsoidal aspect (Fig. 6*A*). Similar morphological changes also were found in hindleg quadriceps endplates and in anterior tibialis muscles (not shown).

NMJ ultrastructure in transgenic animals was highly variable. Although the mean length of postsynaptic membrane folds was similar among transgenics and controls ($0.6 \pm 0.05 \mu\text{m}/\mu\text{m}$ synapse length), only 7 of 16 analyzed NMJs from transgenic mice as compared with 11 of 14 NMJs in control mice possessed average-length postsynaptic folds (Fig. 6*B*, *Top*). The remaining transgenic NMJs displayed either of two pathological features, both reported in NMJs of aged humans (20). One-fourth of the NMJs in transgenic mice as compared with 7% of control NMJs presented highly exaggerated, branched and densely packed postsynaptic folds, similar to those occurring in the Eaton-Lambert syndrome (21) (average of $0.87 \pm 0.16 \mu\text{m}$, Fig. 6*B*, *Middle*). The remaining third of the transgenic NMJs, but only 14% of control NMJs, possessed short, ablated postsynaptic folds ($0.30 \pm 0.07 \mu\text{m}$, Fig. 6*B*, *Bottom*), which resembled those of myasthenia gravis patients (22).

Decreased muscle volume and atrophy of muscle fibers in adult transgenic animals were observed in 4-month-old mice. Electron microscopy subsequently indicated general loosening of intracellular structures in transgenic muscle fibers, but not in controls (Fig. 6*C*). Intracellular spaces were filled with large, structureless vacuoles. The distance between myofilaments and between myofibrils was enlarged. Triads of T tubules and terminal cisternae appeared to be dissociated, mitochondria were no longer aligned with I bands of the sarcolemma and were clearly swollen, with cristae no longer visible (Fig. 6*C*). No NMJ was observed in association with these wasted, damaged muscle regions.

DISCUSSION

We have observed that overexpression of AChE in spinal cord neurons of transgenic mice promotes a persistent, but enigmatic, enlargement of motoneuron perikarya and a severe, delayed-onset neuromotor pathology. The dual cholinergic and noncholinergic properties of AChE raise the possibility that either or both of these activities could be involved in mediating the morphologic transformation of motoneurons and the ultimate demise of NMJs and muscle fibers in adult mice. Enhanced levels of ChAT mRNA in motoneurons of transgenic embryos suggest the existence of a compensatory feedback loop that is sensitive to cholinergic inputs. As ChAT is responsible for synthesizing ACh, hyperactivation of ChAT gene expression in spinal cord motoneurons of transgenic embryos could increase available ACh and stabilize cholin-

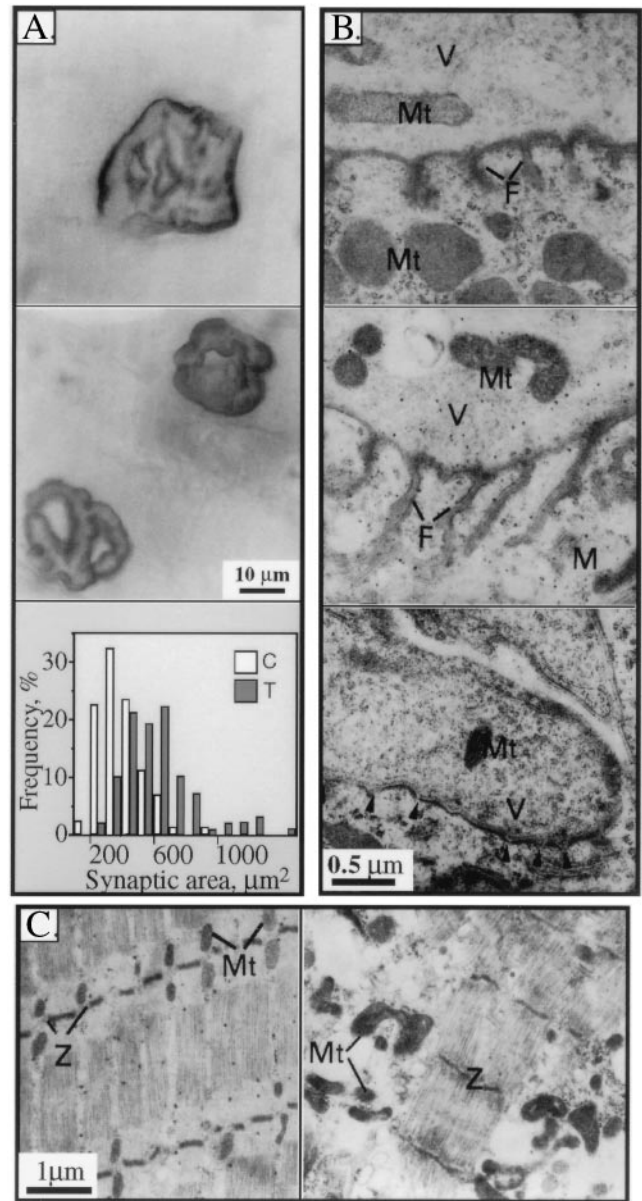


FIG. 6. Enlargement and shape modifications in diaphragm neuromuscular junctions of transgenic animals. (*A*) NMJ surface changes. Wholemount cytochemical staining of AChE activity was performed on fixed diaphragms from 4-month-old transgenic (*Top*) and control (*Middle*) animals. Transgenic NMJs displayed larger circumference and fading boundaries as compared with the complex, sharp contours in controls. Representative endplates from 12 control and transgenic mice. Similar results were obtained using methylene blue staining for total proteins (not shown). (*Bottom*) Stained areas in μm^2 for motor endplates illustrated above (for 90 control, 100 transgenic terminals) are presented as a frequency distribution plot. (*B*) Postsynaptic fold changes. Electron microscopy of 80-nm crosssections of terminal diaphragm zones reveals variable deformities in NMJ from transgenic mice. (*Top*) Normal NMJ. (*Middle*) Transgenic NMJ with exaggerated postsynaptic folds. (*Bottom*) Transgenic NMJ with short, undeveloped folds marked by arrowheads. V, vesicles; M, muscle; F, postsynaptic folds. (*C*) Muscle abnormalities. (*Left*) Longitudinal section from normal diaphragm muscle. Note the organization of mitochondria (Mt) at well-aligned Z bands (Z). (*Right*) Transgenic diaphragm muscle with fiber atrophy, loss of muscle fiber organization, and swelling of mitochondria at disrupted Z bands.

ergic circuitry under conditions of AChE overexpression. In contrast, suppressed levels of mRNA encoding the cell surface protein neurexin I β in spinal cord of embryonic and newborn mice should change neurexin-neuroligin interactions, possibly

affecting both perikarya and synapse properties. This may tentatively hint at the activation of a feedback pathway that is responsive to the noncatalytic activities of AChE and attribute physiological significance to the homology between AChE and the neuroligin-related cell surface proteins, purported to be involved in cell adhesion and synaptogenic interactions in the nervous system. The postnatal normalization we observed in the levels of both ChAT and neuroligin β mRNAs implies a temporally restricted window during which motoneurons can recruit these two feedback loops. The delayed onset of neuromuscular pathologies, as compared with apparently normal embryonic development, thus may reflect the cumulative damage resulting from this irretrievable loss of neuronal transcriptional plasticity.

In light of a previous report that motoneurons contribute synaptic AChE to the amphibian NMJ (19), and assuming that NMJs represent less than 0.1% of the muscle surface (23), the 6% fraction of human enzyme we observed in extracts from muscle not itself expressing the transgene likely reflects a significant accumulation of motoneuron-derived transgenic enzyme in the synapse. This is not surprising as we previously noted that levels of synaptic AChE were elevated ≥ 5 -fold in NMJs from *Xenopus* embryos overexpressing this same cDNA and in which the corresponding nerve terminals were stained for active enzyme (4, 5). Therefore, the disastrous long-term effects of overexpressed AChE could be tentatively attributed, to chronic disturbances in cholinergic neurotransmission. Impaired cholinergic transmission is indeed associated with several congenital and acquired amyotrophic diseases characterized by progressive, juvenile- or adult-onset neuromotor deterioration. Eaton-Lambert syndrome is associated with malfunctioning presynaptic calcium channels and suppressed ACh release (21), myasthenia gravis involves autoimmune suppression of muscle nicotinic acetylcholine receptors (22), and amyotrophic lateral sclerosis results from motoneuron death (24). However, while our findings demonstrate that a moderate, but stable, increase in motoneuron expression of AChE is sufficient to predispose mouse NMJs and muscle to late-onset progressive deterioration, it is not clear whether such deterioration is due to abnormal neuronal inputs, the presence of high levels of AChE in the synapse, or other reasons. Moreover, the severity of the neuromotor degenerative phenotype is difficult to explain solely in terms of cholinergic dysfunction. Rather, it likely represents the outcome of accumulated damage due to various secondary and tertiary changes in additional nerve and/or muscle components.

The morphogenic potency of AChE has now been well established in diverse cell culture models. A neurite outgrowth-promoting activity was demonstrated for AChE in various cultured chicken neurons and attributed to noncatalytic activities affecting cell adhesion properties (1, 2). In addition, our expression of various alternative human AChE cDNAs in glioma cells (25), as well as in *Xenopus* motoneurons (unpublished data) traced this activity to the synaptic form of the enzyme. The mechanism for noncatalytic AChE morphogenic activities is yet unknown. However, Darboux *et al.* (10) demonstrated that in addition to the primary sequence homologies between neurotactin and AChE, the esterase-like domain in *Drosophila* neurotactin likely shares a striking three-dimensional structural similarity with AChE and that this domain plays a prominent role in the protein's cell adhesion properties. In addition, the recently identified neuroligin family of mammalian neuronal cell surface molecules all contain an extracellular esterase-homologous domain sharing 35% homology with *Torpedo* AChE (7). That the overex-

pression of AChE in spinal cord neurons is associated with a specific suppression in the levels of neuroligin β mRNA during embryonic development is highly suggestive of a role for AChE in the neuroligin-neurexin paradigm of cell recognition events. If so, the spatiotemporally coordinated expression of AChE and neurexins in the embryonic spinal cord during normal development, together with the suppression of neuroligin β mRNA levels in AChE-transgenic mice, could reflect a functional, rather than casual association. In that case, our findings would represent *in vivo* indications for a physiologically relevant interaction between AChE and a cell-surface molecule thought to be involved in neuronal development, synaptogenesis, and synapse maintenance.

We thank Drs. S. Seidman and C. Kalcheim (Jerusalem) for helpful discussions and Dr. B. Norgaard-Pedersen (Copenhagen) for antibodies. This work was supported by Grants 17-97-1-7007 from the U.S. Army Medical Research and Defense Command and the U.S.-Israel Binational Science Foundation (to H.S.). C.A. was a recipient of an Institut National de la Santé et de la Recherche Médicale (France) exchange fellowship with the Israel Ministry of Science and Arts. A.F. received a postdoctoral fellowship from the Smith Foundation for Psychobiology.

- Small, D. H., Reed, G., Whitefield, B. & Nurcombe, V. (1995) *J. Neurosci.* **15**, 144–151.
- Layer, P. G. & Willbold, E. (1995) *Prog. Histochem. Cytochem.* **29**, 1–99.
- Jones, S. A., Holmes, C., Budd, T. C. & Greenfield, S. A. (1995) *Cell Tissue Res.* **279**, 323–330.
- Shapira, M., Seidman, S., Sternfeld, M., Timberg, R., Kaufer, D., Patrick, J. & Soreq, H. (1994) *Proc. Natl. Acad. Sci. USA* **91**, 9072–9076.
- Seidman, S., Sternfeld, M., Ben Aziz-Aloya, R., Timberg, R., Kaufer-Nachum, D. & Soreq, H. (1995) *Mol. Cell. Biol.* **14**, 459–473.
- Ichichtenko, K., Hata, Y., Nguyen, T., Ullrich, B., Missler, M., Moomaw, C. & Sudhof, T. C. (1995) *Cell* **81**, 435–443.
- Ichichtenko, K., Nguyen, T. & Sudhof, T. C. (1996) *J. Biol. Chem.* **271**, 2676–2682.
- Barthalay, Y., Hipeau-Jacquotte, R., Escalera, S., Jimenez, F. & Piovant, M. (1990) *EMBO J.* **9**, 3603–3609.
- Auld, V. J., Fetter, R. D., Broadie, K. & Goodman, C. S. (1995) *Cell* **81**, 757–767.
- Darboux, I., Barthalay, Y., Piovant, M. & Hipeau-Jacquotte, R. (1996) *EMBO J.* **15**, 4835–4843.
- Ushkaryov, Y. A., Petrendo, A. G., Geppert, M. & Sudhof, T. C. (1992) *Science* **257**, 50–56.
- Ullrich, B., Ushkaryov, Y. A. & Sudhof, T. C. (1995) *Neuron* **14**, 497–507.
- Puschell, A. W. & Betz, H. (1995) *J. Neurosci.* **15**, 2849–2856.
- Beeri, R., Andres, C., Lev-Lehman, E., Timberg, R., Huberman, T., Shani, M. & Soreq, H. (1995) *Curr. Biol.* **5**, 1063–1071.
- Rachinsky, T. L., Camp, S., Li, Y., Ekstrom, T. J., Newton, M. & Taylor, P. (1990) *Neuron* **5**, 317–327.
- Misawa, H., Ishii, K. & Deguchi, T. (1992) *J. Biol. Chem.* **267**, 20392–20399.
- Lev-Lehman, E., Deutch, V., Eldor, A. & Soreq, H. (1997) *Blood* **89**, 3644–3653.
- Li, Y., Camp, S. & Taylor P. (1993) *J. Biol. Chem.* **268**, 5790–5795.
- Anglister, L. (1991) *Cell Biol.* **115**, 755–764.
- Wokke, L. H. J., Jennekens, F. G. I., van den Oord, C. J. M., Veldman, H., Smith, L. M. E. & Leppink, G. J. (1990) *J. Neurol. Sci.* **95**, 291–310.
- Lambert, E. H. & Elmqvist, D. (1971) *Ann. N.Y. Acad. Sci.* **183**, 183–199.
- Engel, A. G. & Santa, T. (1971) *Ann. N.Y. Acad. Sci.* **183**, 46–63.
- Hall, Z. & Sanes, J. R. (1973) *Cell* **72**, 99–121.
- Robert, H. & Brown, G., Jr. (1995) *Cell* **80**, 687–692.
- Karpel, R., Sternfeld, M., Ginzberg, D., Guhl, E., Graessman, A. & Soreq, H. (1996) *J. Neurochem.* **66**, 114–123.